Published in final edited form as:
Curr Biol. 2009 May 12; 19(9): 768–773. doi:10.1016/j.cub.2009.03.022.

Bcl-2 proteins EGL-1 and CED-9 do not regulate mitochondrial fission or fusion in *Caenorhabditis elegans*

David G. Breckenridge[1,*,#], **Byung-Ho Kang**[2,#], and **Ding Xue**[1,*]

[1]Department of Molecular, Cellular and Developmental Biology, University of Colorado, Boulder, Colorado 80309, USA

[2]Department of Microbiology and Cell Science, Interdisciplinary Center for Biotechnology Research, University of Florida, Gainesville, Florida 32611, USA

SUMMARY

The Bcl-2 family proteins are critical apoptosis regulators that associate with mitochondria and control the activation of caspases. Recently, both mammalian and *C. elegans* Bcl-2 proteins have been implicated in controlling mitochondrial fusion and fission processes in both living and apoptotic cells. To better understand the potential roles of Bcl-2 family proteins in regulating mitochondrial dynamics, we carried out a detailed analysis of mitochondria in animals that either lose or have increased activity of *egl-1* and *ced-9*, two Bcl-2 family genes that induce and inhibit apoptosis in *C. elegans*, respectively. Unexpectedly, we found that loss of *egl-1* or *ced-9*, or overexpression of their gene products, had no apparent effect on mitochondrial connectivity or mitochondrial size. Moreover, loss of *ced-9* did not affect the mitochondrial morphology observed in a *drp-1* mutant, where mitochondrial fusion occurs but mitochondrial fission is defective, or in a *fzo-1* mutant, where mitochondrial fission occurs but mitochondrial fusion is restricted, suggesting that *ced-9* is not required for either the mitochondrial fission or fusion process in *C. elegans*. Taken together, our results argue against an evolutionarily conserved role for Bcl-2 proteins in regulating mitochondrial fission and fusion.

RESULTS

Mitochondrial morphogenesis is not affected in *egl-1(lf)* or *ced-9(lf)* mutants

Recently, the *C. elegans* pro-apoptotic BH3-only Bcl-2 protein EGL-1 has been implicated in promoting mitochondria fission during apoptosis [1]. In addition, the *C. elegans* anti-apoptotic Bcl-2 protein CED-9 was shown to mediate mitochondria fission during apoptosis in one study [1] but was found to promote mitochondria fusion in healthy cells in another [2], calling into question of the exact physiological roles of *C. elegans* Bcl-2 family proteins in regulating mitochondria dynamics. To address the critical issue of whether Bcl-2 proteins regulate normal mitochondrial fission or fusion process in *C. elegans*, we carried out a comprehensive analysis of mitochondria morphology and structure in animals that either lose or have increased activity of *egl-1* or *ced-9*. First, we visualized mitochondria in early *C. elegans* embryos that were

*Correspondence: Dr. David Breckenridge, breckenridge.david@gmail.com, Dr. Ding Xue, ding.xue@colorado.edu.
#These two authors contributed equally to the work.

stained with the mitochondria specific dye, tetramethylrhodamine ethyl ester (TMRE); the large blastomere size in early embryos permits clear visualization of the mitochondrial network. In N2 (wild type) animals, where mitochondrial fission and fusion processes are balanced, mitochondria appeared as a large network, evenly distributed through out each cell (Figure 1A) [1,3–7]. In *drp-1(tm1108)* mutant animals, which are null for the DRP-1 protein expression and defective in mitochondrial fission [7], mitochondria appeared as highly connected clusters and asymmetrically distributed in individual blastomeres (Figure 1B), which results from ongoing mitochondrial fusion in the absence of mitochondrial fission [6]. In contrast, in *fzo-1(tm1133)* animals, which harbor a deletion in the *fzo-1* gene and where mitochondrial fusion is compromised but mitochondrial fission continues [7], the mitochondrial network was disrupted into highly fragmented, punctiform organelles (Figure 1C). Thus, a defect in either the mitochondrial fission or fusion process is clearly identifiable in this assay.

Mitochondria in *egl-1(n3082)* animals, which carry a strong loss-of-function (*lf*) mutation in *egl-1*, appeared undistinguishable from those in wild type animals (Figure 1D), although somatic programmed cell death is abolished in these animals [8]. Similarly, the mitochondrial network appeared unaffected in *ced-9(n1950gf)* animals (Figure 1E), which carry a gain-of-function (*gf*) mutation (a G169E substitution) in the *ced-9* gene that prevents EGL-1 from binding to CED-9 [9, 10] and thus blocks *C. elegans* programmed cell death [11]. We also analyzed mitochondria morphology in two *ced-9(lf)* mutants: *ced-9(n1653ts)* and *ced-9 (n2812)*. The *n1653* mutation causes a Y149N substitution in CED-9 that reduces its association with CED-4 at the restrictive temperature (25°C) and compromises its apoptosis inhibitory activity [12], leading to ectopic apoptosis. *n2812* results in an early nonsense mutation in the *ced-9* gene [13] that abolishes expression of *ced-9* in *C. elegans* [14] and is a putative null allele. *ced-9(n282)* animals are embryonic lethal due to excessive apoptosis but can be maintained and analyzed in the *ced-3(lf)* or *ced-4(lf)* mutant background, which blocks apoptosis [11]. As shown in Figure 1F–H, we observed no significant difference in mitochondrial morphology in *ced-9(n1653ts), ced-4(n1162) ced-9(n2812),* or *ced-9(n2812); ced-3(n717)* embryos compared to that in N2 embryos or that in *ced-3(n717)* or *ced-4 (n1162)* embryos or *ced-9(n1653ts)* embryos at the permissive temperature (Figure S1). We quantified the connectivity of mitochondria in N2, *drp-1(tm1108), fzo-1(tm1133), egl-1 (n3082),* and *ced-9(n2812); ced-3(n717)* blastomeres by generating line intensity plots and calculating the frequency of major TMRE fluorescent spikes (Figure S2; method described in Experimental Procedures). In N2 blastomeres, TMRE fluorescent signals varied in frequency, with an average of 0.49 fluorescent spikes/μm (Figure S2). TMRE fluorescent signals were very broad and of low spike frequency in *drp-1(tm1108)* blastomeres (average frequency of 0.16 fluorescent spikes/μm; Figure S2), consistent with large clumps of mitochondria asymmetrically distributed within cells. In contrast, *fzo-1(tm1133)* embryos displayed high frequency of TMRE signal spikes, averaging 2.29 spikes/μm, delineating punctiform mitochondria evenly distributed throughout the cells (Figure S2). The frequency of TMRE signal spikes in *egl-1(n3082), ced-9(n1950gf),* or *ced-9(n2812); ced-3(n717)* blastomeres was similar to that of N2 animals [an average frequency of 0.44 spikes/μm and 0.48 spikes/μm in *egl-1(n3082)* and *ced-9(n2812); ced-3(n717)* blastomeres; Figure S2]. Taken together, these results suggest that loss of *egl-1* or *ced-9 function* does not affect mitochondria dynamics and morphology in *C. elegans*

Of note, a recent report showed that mitochondria appeared highly fragmented in *ced-9 (n1653ts)* embryos at the restrictive temperature [2]. However, in that study, embryos were examined at a later stage of development and the mitochondrial fragmentation observed could have been the result of widespread ectopic apoptosis [1,7], rather than a requirement for *ced-9* to maintain the integrity of the mitochondrial network. Importantly, CED-9 protein is ubiquitously expressed in embryos as early as the two cell stage [14]. If CED-9 is required to

maintain normal mitochondrial networks, its role should be uncovered in early embryos. The expression pattern of EGL-1 is not well understood, but *egl-1* transcription has been shown to be upregulated in several cells destined to die [15]. Nonetheless, our results suggest that the activity *of egl-1* is not required for normal mitochondrial morphogenesis.

We carried out electron microscopy (EM) analysis to confirm the TMRE staining results in Figure 1 and to investigate whether *egl-1* or *ced-9* might play subtle roles in regulating mitochondrial dynamics. In 2-dimensional images of EM sections from N2 embryos, mitochondria appeared in a variety of shapes and sizes, ranging from small spherical organelles to longer dumbbell shaped organelles (Figure 2A), and with a mean longitudinal length of 0.94 μm (Figure 2F). As expected, mitochondria in *drp-1(tm1108)* embryos were very long, with fewer individual mitochondria observed in each cell (Figure S3A) and a mean mitochondrial length of 2.28 μm (Figure 2F)[7]. *fzo-1(tm1133)* embryos displayed only small and spherical mitochondria, with a mean mitochondrial length of 0.38 μm (Figure S3B and Figure 2F). However, mitochondria in *egl-1(n3082), ced-9(n1950gf), ced-9(n1653ts),* and *ced-9(n2812); ced-3(n717)* embryos appeared similar to those observed in N2 embryos and in all cases had mean longitudinal mitochondrial lengths that were not significantly different from that of N2 animals (Figure 2B–E). Mitochondria in the germline, gut, and muscle cells of adult *egl-1(lf), ced-9(lf); ced-3(lf),* or *ced-9(gf)* mutants also appeared normal (data not shown). The mitochondrial morphology in N2, *drp-1(tm1108), fzo-1(tm1133), egl-1(n3082),* and *ced-9 (n2812); ced-3(n717)* animals was confirmed by serial EM sectioning and 3-dimensional reconstruction from the serial images (Figure 3 and Figure S4). Again, mitochondria in N2, *egl-1(n2812),* and *ced-9(n2812); ced-3(n717)* animals varied in shape and size and were evenly distributed throughout the cell. In contrast, mitochondria in *drp-1(tm1108)* embryos were long, highly interconnected, and clustered around the nucleus, whereas mitochondria in *fzo-1 (tm1133)* embryos were small, puntiform, and evenly distributed. Altogether, these results confirm that *egl-1* and *ced-9* do not have a detectable role in regulating mitochondrial fission or fusion in *C. elegans*.

ced-9 does not promote *drp-1*-dependent mitochondrial fission or *fzo-1*-dependent mitochondrial fusion

If CED-9 somehow has both pro-fission and pro-fusion activities as previously reported [1, 2], it is conceivable that loss of *ced-9* in *C. elegans* would yield no net effect on the mitochondrial network. To address this possibility, we examined the effect of a *ced-9(lf)* mutation on the mitochondrial morphologies in *drp-1(tm1108)* and *fzo-1(tm1133)* mutant backgrounds, where mitochondrial fusion or fission occurs in isolation, respectively [5]. Mitochondria in *fzo-1(tm1133); ced-4(n1162) ced-9(n2812)* triple mutant embryos appeared highly fragmented and indistinguishable from mitochondria in *fzo-1(tm1133); ced-4(n1162)* or *fzo-1(tm1133)* embryos (Figure 1C and J, and data not shown). On the other hand, mitochondria in *ced-4(n1162) ced-9(n2812); drp-1(tm1108)* triple mutants were highly connected and asymmetrically distributed in the cells, just as was observed in *ced-4(n1162); drp-1(tm1108)* and *drp-1(tm1108)* animals (Figure 1B and I, and data not shown). Therefore, in a physiological setting (i.e. where *ced-9*, *drp-1*, and *fzo-1* are not overexpressed), loss of *ced-9* has no discernable effect on either *drp-1*-dependent mitochondrial fission or *fzo-1*-dependent mitochondrial fusion. In comparison, *drp-1(tm1108)* completely suppresses the highly fragmented mitochondria phenotype caused by the *fzo-1(tm1133)* mutation [7], indicating that *drp-1* is required for the mitochondrial fragmentation observed in *fzo-1* mutants.

Overexpression of CED-9 or EGL-1 does not promote mitochondrial fission or fusion

Although *egl-1* and *ced-9* are not required for mitochondrial fission or fusion in normal cells, they might directly affect one of these processes during apoptosis [1]. Therefore, we examined whether overexpression of either EGL-1 or CED-9 could affect mitochondrial morphology in

C. elegans, in comparison with their activities in inducing or inhibiting apoptosis. We generated animals carrying an integrated transgene of *egl-1* or *ced-9* under the control of heat-shock promoters (P $_{hsp}$*egl-1* and P $_{hsp}$*ced-9*, respectively) and examined the mitochondrial network in young embryos before and after heat-shock treatment. Since overexpression of EGL-1 potently induces ectopic apoptosis in *C. elegans* [8] and overexpression of CED-9 strongly inhibits normal programmed cell death [13], we quantified the effect of induced overexpression of EGL-1 and CED-9 on cell death by counting the number of cell corpses in heat-treated P$_{hsp}$*egl-1* and P$_{hsp}$*ced-9* embryos and the number of cells that should die but inappropriately survived in the anterior pharynx of larvae that hatched from the heat-treated P$_{hsp}$*ced-9* embryos. Heat-shock treatment of P$_{hsp}$*egl-1* embryos resulted in the appearance of over 40 cell corpses by the comma stage of embryonic development (Figure 4A) and ultimately caused growth arrest and death of all embryos prior to hatching (data not shown). In contrast, heat-shock treatment of P$_{hsp}$*ced-9* animals greatly reduced the number of cell corpses in embryos (Figure 4A) and caused on average the survival of over nine extra cells in the anterior pharynx of the resulting larvae (Figure 4B). These results demonstrate that induced global expression of EGL-1 and CED-9 potently promotes or inhibits apoptosis in P$_{hsp}$*egl-1* and P$_{hsp}$*ced-9* animals, respectively. However, we did not observe an obvious change in mitochondrial morphology in P$_{hsp}$*egl-1* or P$_{hsp}$*ced-9* embryos following the heat shock treatment (Figure 4C). In contrast, *drp-1(tm1108)* or *fzo-1(tm1133)* embryos at the same developmental stage showed clear signs of mitochondrial clustering and mitochondrial fragmentation, respectively (Figure S5). Analysis of EM micrographs of heat-treated P$_{hsp}$*egl-1* embryos revealed that in most cells mitochondria appeared normal (Figure 4D) and that the mean mitochondrial length remained at 0.92 μm, similar to what was observed in N2 animals (Figure 2F). Highly fragmented and spherical mitochondria were observed in cell corpses of P$_{hsp}$*egl-1* embryos (Figure 4E), suggesting that mitochondria eventually fragment in dying cells, probably as a secondary event of apoptosis. Consistent with this, we did not observe evidence of widespread mitochondrial fragmentation or ectopic apoptosis when EGL-1 was overexpressed in a *ced-3(lf)* background, even when animals were observed up to five hours post heat-shock treatment (Figure S6; data now shown). Therefore, elevated levels of EGL-1 and CED-9 proteins do not appear to directly promote either mitochondrial fission or fusion in *C. elegans*. However, our results do not rule out the possibility that EGL-1 may play a role in promoting mitochondria fragmentation in normally dying cells. Of note, it was reported that ectopic *egl-1* expression (using a similar P$_{hsp}$*egl-1* construct) induced widespread mitochondrial fission, independent of *ced-3* [1]. The reason for the discrepancy between that study and ours is currently unclear.

DISCUSSION

Although several recent reports have suggested a connection between Bcl-2 proteins and the mitochondrial fission or fusion process [1,2,16–18], we did not find an obvious requirement for *egl-1* or *ced-9* in regulating either process in *C. elegans*. Analysis of strong loss-of-function *egl-1* and *ced-9* mutants and a gain-of-function *ced-9* mutant, which either are defective in apoptosis or contain excessive cell deaths, revealed no detectable difference in the mitochondrial network when observed in live animals stained with mitochondria-specific dye, in high magnification EM sections, or in 3-dimensional models reconstructed from serial EM sections. Moreover, *ced-9* does not affect either *drp-1*-dependent mitochondrial fission or *fzo-1*-dependent mitochondrial fusion *in vivo* (Figure 1B, C, I, J). These findings disagree with two recent reports that proposed a role for EGL-1 and CED-9 in regulating mitochondrial dynamics in *C. elegans* [1,2]. In one report, overexpression of EGL-1 was shown to induce mitochondrial fragmentation, independent of *ced-3*, and mitochondrial fission induced by ectopic *drp-1* expression was blocked by both *ced-9(n1950gf)* and *ced-9(n2812lf)* mutations [1]. However, we did not observe widespread mitochondrial fragmentation following EGL-1 induction (Figure 4) and loss of *ced-9* does not affect mitochondria fission or fusion on its own or affect *drp-1*-dependent mitochondrial fission when examined in a physiological context (i.e.

in the *fzo-1* mutant background when *drp-1* was not overexpressed) (Figure 1C, J). Mitochondria are fragmented in cell corpses following EGL-1 induction, but this is likely the result of a downstream caspase-dependent apoptotic process [7] rather than a process that is regulated by EGL-1 or CED-9 to activate apoptosis. Indeed, we did not detect any obvious cell death defect in the strong loss-of-function *drp-1(tm1108)* mutant, where mitochondria are highly fused, or in animals deficient in *fzo-1* or *eat-3*, where mitochondria are highly fragmented [7], indicating that the mitochondria fusion or fission process does not play a role in apoptosis activation. Similarly, we found that overexpression of CED-9 in *C. elegans* does not induce mitochondrial fission or fusion, although its overexpression was reported to cause excessive mitochondrial fusion in cultured mammalian cells [2]. CED-9 therefore may target proteins or signaling pathways in mammals that don't exist in the worm. Taken together, our findings indicate that EGL-1 and CED-9 do not have a discernable role in promoting either mitochondrial fission or fusion in *C. elegans* and challenge the hypothesis that regulation of mitochondrial morphogenesis is an evolutionarily conserved feature of Bcl-2 proteins [2].

In mammals, overexpression of Bcl-xL can induce both mitochondrial fission and fusion depending on its level of expression [2,17] and can increase mitochondrial biomass [17], whereas overexpression of Bcl-2 promotes mitochondrial fusion [2] and overexpression of Bax induces mitochondrial fission and apoptosis [16]. Paradoxically, Bax and Bak are also reported to be important for mitochondrial fusion in healthy cells [18], raising an interesting question of how mammalian Bcl-2 proteins achieve opposing functions in mitochondria dynamics. Bcl-2 proteins might affect mitochondria fusion or fission in mammals by interacting with the mitochondrial fusion machinery, since Bcl-xL was shown to interact with Mfn2 [2] and Bax/Bak were found to be required for Mfn2 to form discrete foci in the outer mitochondrial membrane [18]. Therefore, it appears that mammalian Bcl-2 proteins may have evolved a role to directly or indirectly regulate mitochondrial fission/fusion and such a role does not appear to exist in their worm counterparts. Further analysis of mitochondria dynamics under physiological settings will be critical to understand the roles and mechanisms of mammalian Bcl-2 proteins in regulating mitochondria fusion/fission.

Supplementary Material

Refer to Web version on PubMed Central for supplementary material.

ACKNOWLEDGEMENTS

We thank *Caenorhabditis* Genetics Center for strains and Tom Giddings for assistance with EM operation. This research was supported in part by fellowships from the Jane Coffins Child Memorial Fund for Medical Research and the Canadian Institutes of Health Research (D.G.B), start-up funds from the University of Florida (B.H.K), the Burroughs Wellcome Fund Career Award (D.X.), and the NIH R01 GM059083 and GM079097 grants (D.X.).

REFERENCES

1. Jagasia R, Grote P, Westermann B, Conradt B. DRP-1-mediated mitochondrial fragmentation during EGL-1-induced cell death in *C. elegans*. Nature 2005;433:754–760. [PubMed: 15716954]
2. Delivani P, Adrain C, Taylor RC, Duriez PJ, Martin SJ. Role for CED-9 and EGL-1 as regulators of mitochondrial fission and fusion dynamics. Mol. Cell 2006;21:761–773. [PubMed: 16543146]
3. Ichishita R, Tanaka K, Sugiura Y, Sayano T, Mihara K, Oka T. An RNAi screen for mitochondrial proteins required to maintain the morphology of the organelle in *C. elegans*. J. Biochem 2008;143:449–454. [PubMed: 18174190]
4. Chan DC. Mitochondrial fusion and fission in mammals. Annu. Rev. Cell. Dev. Biol 2006;22:79–99. [PubMed: 16704336]
5. Okamoto K, Shaw JM. Mitochondrial morphology and dynamics in yeast and multicellular eukaryotes. Annu. Rev. Genet 2005;39:503–536. [PubMed: 16285870]

6. Labrousse AM, Zappaterra MD, Rube DA, van der Bliek AM. *C. elegans* dynamin-related protein DRP-1 controls severing of the mitochondrial outer membrane. Mol. Cell 1999;4:815–826. [PubMed: 10619028]
7. Breckenridge DG, Kang B-H, Kokel DK, Mitani S, Staehelin LA, Xue D. *Caenorhabditis elegans drp-1* and *fis-2* regulate distinct cell death execution pathways downstream of *ced-3* and independent of *ced-9*. Mol. Cell 2008;31:586–597. [PubMed: 18722182]
8. Conradt B, Horvitz HR. The *C. elegans* protein EGL-1 is required for programmed cell death and interacts with the Bcl-2-like protein CED-9. Cell 1998;93:519–529. [PubMed: 9604928]
9. Hengartner MO, Horvitz HR. Activation of *C. elegans* cell death protein CED-9 by an amino-acid substitution in a domain conserved in Bcl-2. Nature 1994;369:318–320. [PubMed: 7910376]
10. Parrish J, Metters H, Chen L, Xue D. Demonstration of the in vivo interaction of key cell death regulators by structure-based design of secondsite suppressors. Proc. Natl. Acad. Sci U.S.A 2000;97:11916–11921. [PubMed: 11027303]
11. Hengartner MO, Ellis RE, Horvitz HR. *Caenorhabditis elegans* gene ced-9 protects cells from programmed cell death. Nature 1992;356:494–499. [PubMed: 1560823]
12. Spector MS, Desnoyers S, Hoeppner DJ, Hengartner MO. Interaction between the *C. elegans* cell-death regulators CED-9 and CED-4. Nature 1997;385:653–656. [PubMed: 9024666]
13. Hengartner MO, Horvitz HR. *C. elegans* cell survival gene *ced-9* encodes a functional homolog of the mammalian proto-oncogene bcl-2. Cell 1994;76:665–676. [PubMed: 7907274]
14. Chen F, Hersh BM, Conradt B, Zhou Z, Riemer D, Gruenbaum Y, Horvitz HR. Translocation of *C. elegans* CED-4 to nuclear membranes during programmed cell death. Science 2000;287:1485–1489. [PubMed: 10688797]
15. Peden E, Killian D, Xue D. Cell death specification in *C. elegans*. Cell Cycle 2008;7:2479–2484. [PubMed: 18719375]
16. Karbowski M, Lee YJ, Gaume B, Jeong SY, Frank S, Nechushtan A, Santel A, Fuller M, Smith CL, Youle RJ. Spatial and temporal association of Bax with mitochondrial fission sites, Drp1, and Mfn2 during apoptosis. J. Cell Biol 2002;159:931–938. [PubMed: 12499352]
17. Berman SB, Chen Y-B, Qi B, McCaffery JM, Rucker EB, Goebbels S, Nave KA, Arnold BA, Jonas EA, Pineda Fj, Hardwick MJ. Bcl-xL increases mitochondrial fission, fusion, and biomass in neurons. J. Cell. Biol. 2009Published online.
18. Karbowski M, Norris KL, Cleland MM, Jeong SY, Youle RJ. Role of Bax and Bak in mitochondrial morphogenesis. Nature 2006;443:658–662. [PubMed: 17035996]

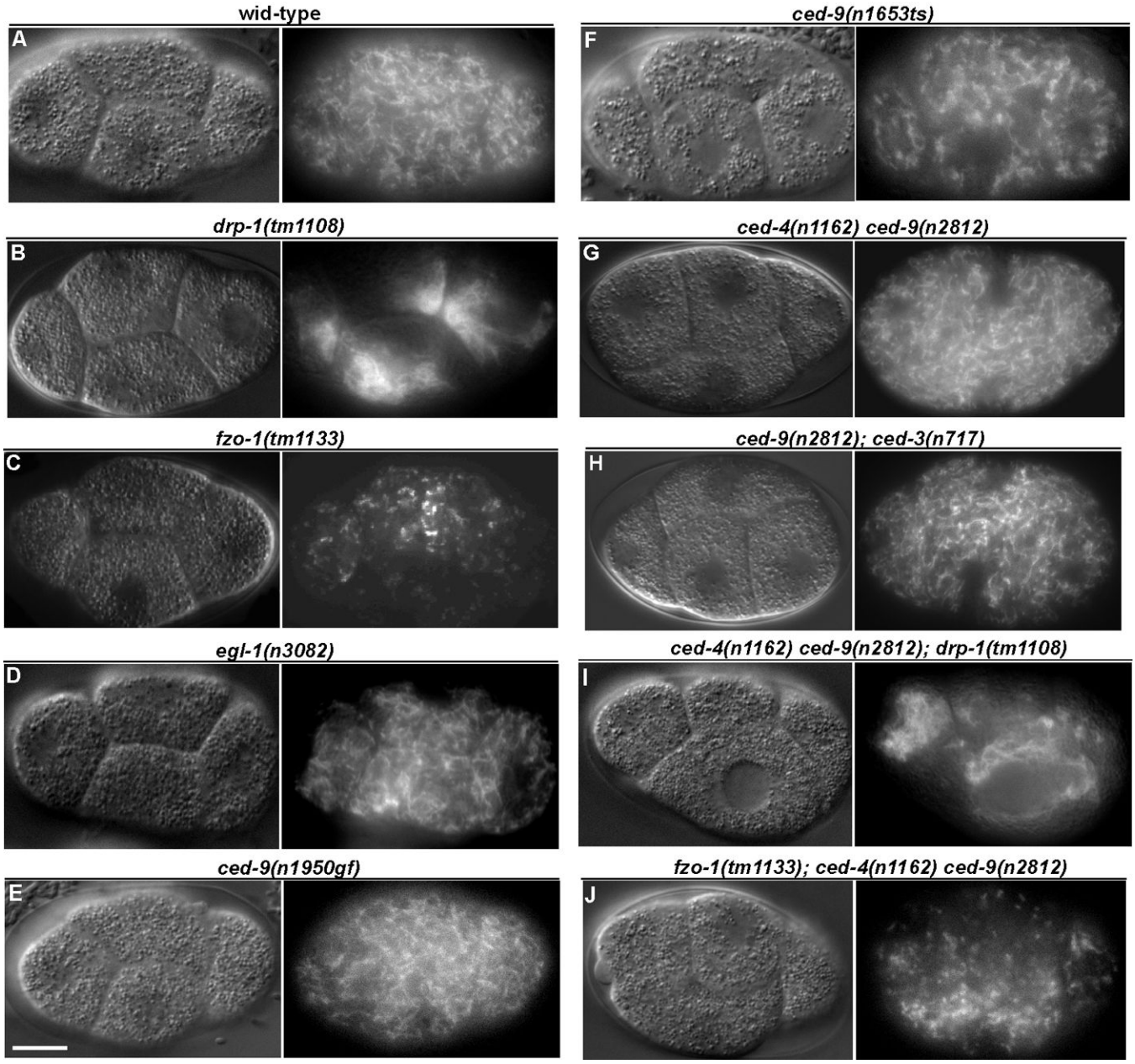

Figure 1.

The mitochondrial network is altered in *fzo-1* and *drp-1* mutants but unaffected by mutations in *egl-1* and *ced-9*. Animals were stained with tetramethylrhodamine ethyl ester (TMRE), a mitochondrial specific dye, and blastomeres at the four-cell embryonic stage were imaged. Embryos were visualized by Differential Interference Contrast (DIC, left) and rhodamine fluorescence (right) microscopy. Representative images are shown. Compared to wild type embryos (A), *drp-1(tm1108)* embryos (B) have a highly connected mitochondrial network, whereas mitochondria appeared highly fragmented in *fzo-1(tm1133)* embryos (C). Mitochondria in *egl-1(n3082)* (D), *ced-9(n1950gf)* (E), *ced-9(n1653ts)* at the restrictive temperature (F), *ced-4(n1162) ced-9(n2812)* (G), and *ced-9(n2812); ced-3(n717)* (H) embryos were indistinguishable from those observed in wild type embryos. Loss of *ced-9* has no effect on the mitochondria morphology in *drp-1(tm1108)* or *fzo-1(tm1133)* animals. The

mitochondrial network in the *ced-4(n1162) ced-9(n2812); drp-1(tm1108)* embryo (I) and in the *fzo-1(tm1133); ced-4(n1162) ced-9(n2812)* embryo (J) is similar to that seen in *drp-1 (tm1108)* embryos (B) and *fzo-1(tm1133)* embryos (C), respectively. Scale bar represents 10 μ m.

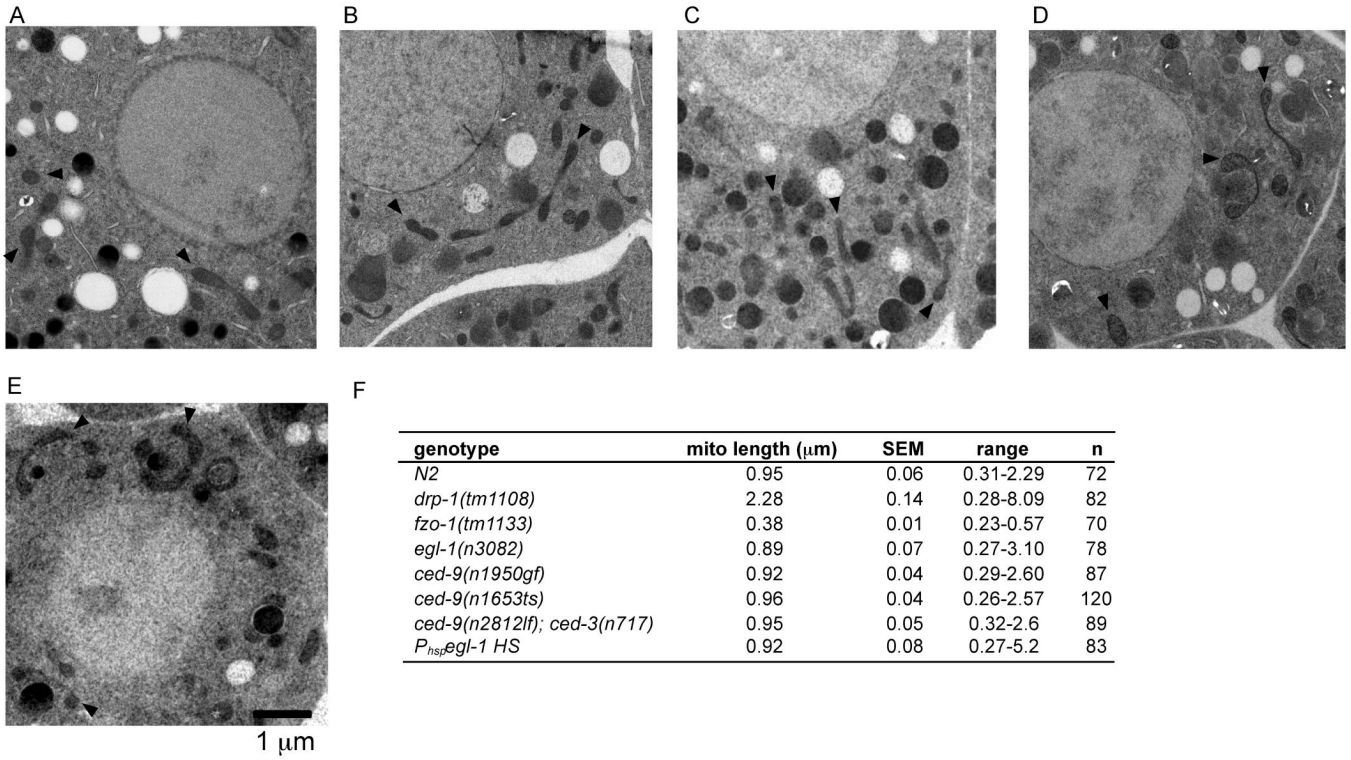

genotype	mito length (μm)	SEM	range	n
N2	0.95	0.06	0.31-2.29	72
drp-1(tm1108)	2.28	0.14	0.28-8.09	82
fzo-1(tm1133)	0.38	0.01	0.23-0.57	70
egl-1(n3082)	0.89	0.07	0.27-3.10	78
ced-9(n1950gf)	0.92	0.04	0.29-2.60	87
ced-9(n1653ts)	0.96	0.04	0.26-2.57	120
ced-9(n2812lf); ced-3(n717)	0.95	0.05	0.32-2.6	89
P_{hsp}*egl-1 HS*	0.92	0.08	0.27-5.2	83

Figure 2.

Electron microscopy (EM) analysis of mitochondria morphology in *egl-1* and *ced-9* mutants. Representative electron micrographs of embryos from the following strains are shown: N2 (A), *egl-1(n3082)* (B), *ced-9(n1950gf)* (C), *ced-9(n1653ts)* at the restrictive temperature (D), *ced-9 (n2812); ced-3(n717)* (E). Scale bar represents 1 μm. Arrows indicate representative mitochondria. (F) Quantification of the mean mitochondrial length. Randomly selected mitochondria from electron micrographs were measured along their longitudinal axis. SEM, standard error of the mean. n, the number of mitochondria scored.

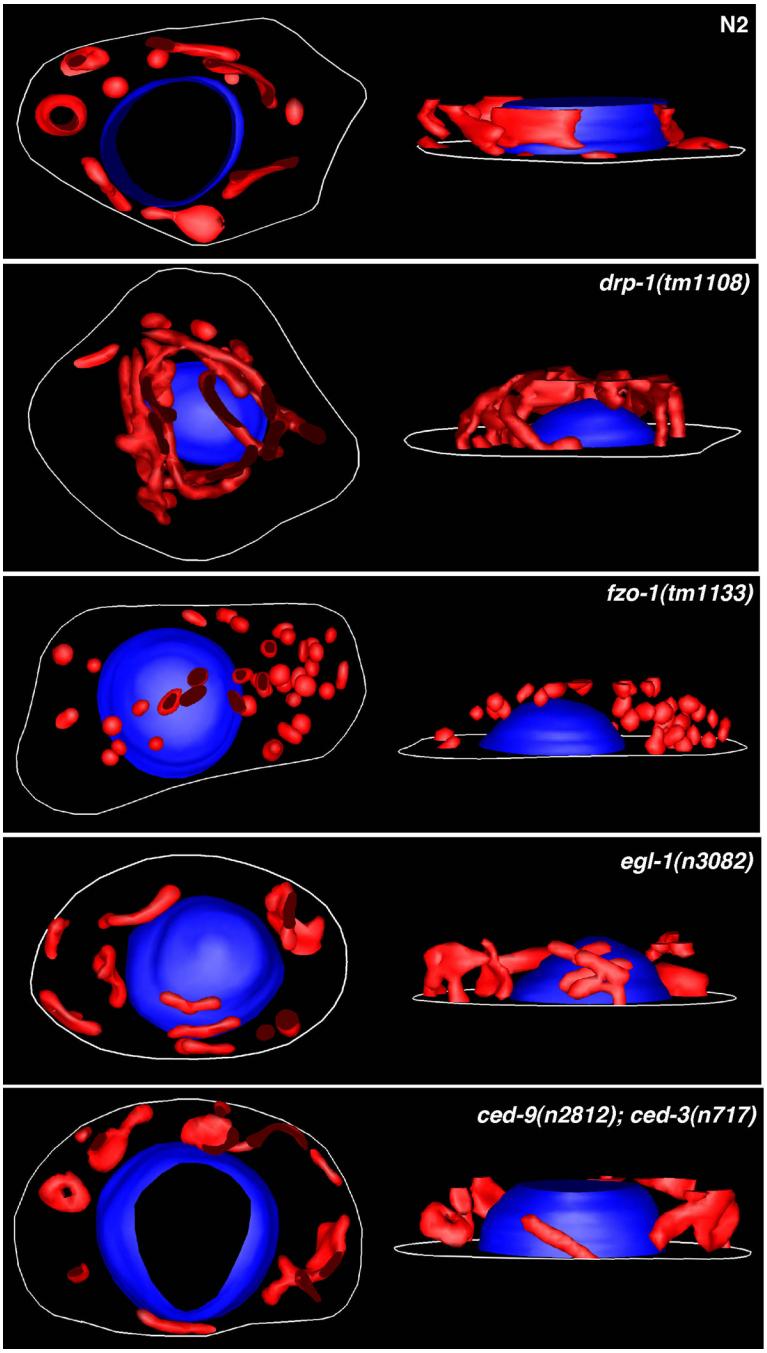

Figure 3.

3-dimensional mitochondria images reconstructed from serial electron micrographs. 3D models of mitochondria (red) in various mutant embryos were generated from stacks consisting of 15~20 serial electron micrographs (10,000X) of 80 nm thick sections (see Experimental Procedures for detail). In each panel, top-down view (left) and side view (right) of the cell are shown. Mitochondria in the *drp-1(tm1108)* mutant are interconnected to form a large network, whereas mitochondria in the *fzo-1(tm1133)* mutant are highly fragmented and spherical. No obvious difference is seen in mitochondria organization and architecture among N2, *egl-1 (n3082)*, and *ced-9(n2812); ced-3(n717)* embryos. Nuclei (blue) and cell outlines (white) are also shown.

A

	Number of Cell Corpses					
	No Heat shock			Heat shock		
genotype	mean	SEM	range	mean	SEM	range
N2	9.77	0.5	7-13	10.4	0.6	7-13
P_{hsp}*ced-9*	8.9	0.5	6-12	0.6	0.2	0-3
P_{hsp}*egl-1*	10.6	0.5	6-14	40.7	2.8	25-61

B

	Number of Extra Cells					
	No Heat shock			Heat shock		
genotype	mean	SEM	range	mean	SEM	range
N2	0.1	0.1	0-1	0.1	0.1	0-1
P_{hsp}*ced-9*	0.2	0.1	0-1	9.4	0.45	6-12

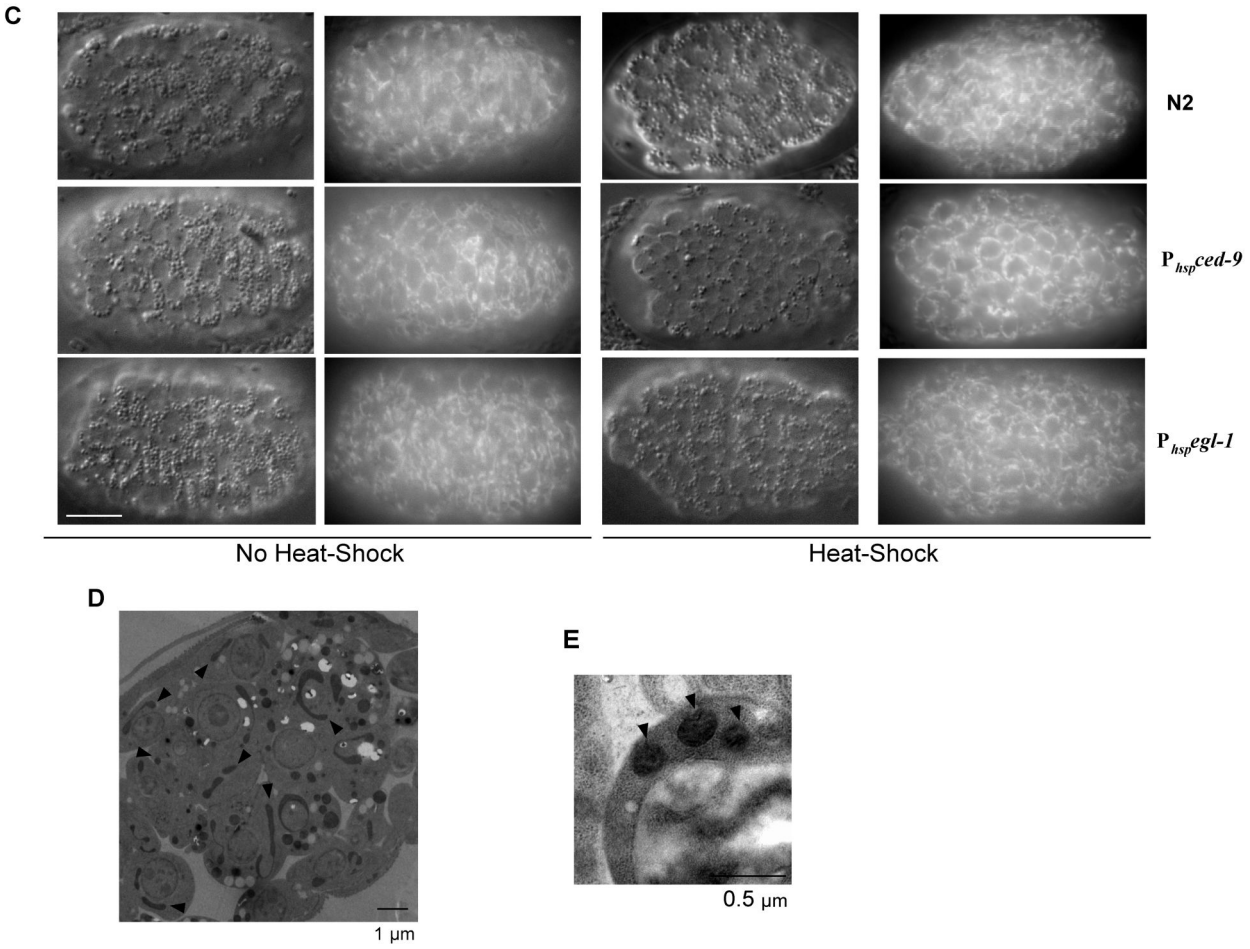

Figure 4.

Overexpression of EGL-1 or CED-9 affects programmed cell death in *C. elegans* but does not obviously affect mitochondrial morphogenesis. (A) N2, P_{hsp}*egl-1 (smIs82)*, or P_{hsp}*ced-9 (smIs157)* embryos were treated with heat-shock (right) or left untreated (left) and the number of cell corpses in the head region of 1.5-fold stage embryos was scored 2 hours post heat-shock treatment. (B) Embryos of the indicated genotypes were treated with heat-shock (right) or left untreated (left) and allowed to hatch into L4 larvae, at which point the number of extra cells that inappropriately survived in the anterior pharynx was scored. 20 animals were scored in both (A) and (B). (C) N2, P_{hsp}*egl-1*, or P_{hsp}*ced-9* embryos were stained with TMRE and either treated with heat-shock (right) or left untreated (left) and visualized by Differential Interference

Contrast (DIC) and rhodamine fluorescence microscopy. Mitochondria in heat-shock treated P_{hsp}*egl-1* or P_{hsp}*ced-9* embryos were indistinguishable from those observed in untreated embryos and wild type embryos. Scale bar represents 10 μm. (D) An EM micrograph of a heat-shock treated P_{hsp}*egl-1* embryo. Arrows indicate several mitochondria of various shapes and sizes. (E) Mitochondria in a cell corpse of a heat-shock treated P_{hsp}*egl-1* embryo are fragmented as a result of apoptosis. SEM: standard error of the mean.